

Ambiguity resolution in SAR interferometry  
by use of three phase centers

Charles V. Jakowatz, Jr., Daniel E. Wahl, Paul A. Thompson

Sandia National Laboratories  
Albuquerque, NM

RECEIVED

MAR 22 1996

OSTI

ABSTRACT

In a typical interferometric synthetic aperture radar (IFSAR) system employed for terrain elevation mapping, terrain height is estimated from phase difference data obtained from two phase centers separated spatially in the cross-track direction. In this paper we show how the judicious design of a three phase center IFSAR renders *phase unwrapping*, i.e., the process of estimating true continuous phases from principal values of phase (wrapped modulo  $2\pi$ ), a much simpler process than that inherent in traditional algorithms. With three phase centers, one IFSAR baseline can be chosen to be relatively small (two of the phase centers close together) so that all of the scene's terrain relief causes less than one cycle of phase difference. This allows computation of a coarse height map without use of any form of phase unwrapping. The cycle number ambiguities in the phase data derived from the other baseline, chosen to be relatively large (two of the phase centers far apart), can then be resolved by reference to the heights computed from the small baseline data. This basic concept of combining phase data from one small and one large baseline to accomplish phase unwrapping has been previously employed in other interferometric problems, e.g., laser interferometry and direction-of-arrival determination from multiple element arrays. The new algorithm is shown to possess a certain form of immunity to corrupted interferometric phase data that is not inherent in traditional two-dimensional path-following phase unwrappers. This is because path-following algorithms must estimate, either implicitly or explicitly, those portions of the IFSAR fringe data where discontinuities in phase occur. Such discontinuities typically arise from noisy phase measurements derived from low radar return areas of the SAR imagery, e.g., shadows, or from areas of steep terrain slope. When wrong estimates are made as to where these phase discontinuities occur, errors in the unwrapped phase values can appear due to the resulting erroneous unwrapping paths. This implies that entire regions of the scene can be reconstructed with incorrect terrain heights. By contrast, since the new method estimates the continuous phase at each point in the image by a straightforward combination of only the wrapped phases from the small and large baseline, phase estimation errors are confined to that point, i.e., errors do not propagate to surrounding pixels. We derive quantitative expressions for the new algorithm that relate the probability of selecting the wrong phase cycle to parameters of the interferometer, e.g., size of the two baselines and phase noise level. We then demonstrate that use of median filtering can very effectively mitigate those cycle errors that do occur. By use of computer simulations, we show how the new algorithm is used to robustly construct terrain elevation maps.

**Keywords:** synthetic aperture radar, SAR, interferometry, IFSAR, phase unwrapping, multiple-baseline interferometry

This work was supported by the United States Department of Energy under Contract DE-AC04-94AL85000.

## 1. INTRODUCTION

In classical SAR interferometry, a phase difference map is computed from the complex SAR image data obtained from a pair of phase centers, as depicted in Figure 1a. This phase difference map, or *fringe image*, represents *principal values* of phase (phase wrapped modulo  $2\pi$ ). The terrain elevation  $h$  at a specified ground location  $(x, y)$  is proportional to the *unwrapped* phase value at that location<sup>1</sup>. An algorithm is therefore required to transform the wrapped phases into unwrapped phases prior to their use in the calculation of the terrain elevation map. A number of solutions to the phase unwrapping problem have been proposed, most of which involve the process called *path following*, which finds paths connecting all pixels along which the phase is assumed to be changing slowly. The challenge here is to determine those portions of the IFSAR fringe map wherein phase discontinuities, resulting either from noisy phase measurements or from overly steep terrain slopes, occur. The unwrapping may then be performed along an appropriate path that does not cross regions of discontinuous data, so that a consistent unwrapped phase result is assured. In any algorithm, however, wrong choices can easily be made as to exactly where the discontinuities lie. The result is that paths might be chosen for unwrapping that *do* cross regions of discontinuous phase, causing errors in the estimated phases to be propagated wherever the path leads, including entire regions of the image.

An alternative solution to the phase unwrapping problem that can mitigate the problems inherent in traditional path following schemes involves insertion of a third phase center into the interferometer, in a manner that creates an additional baseline which is small relative to that formed by the first two phase centers. This geometry is depicted in Figure 1b. The new scheme for height estimation that we

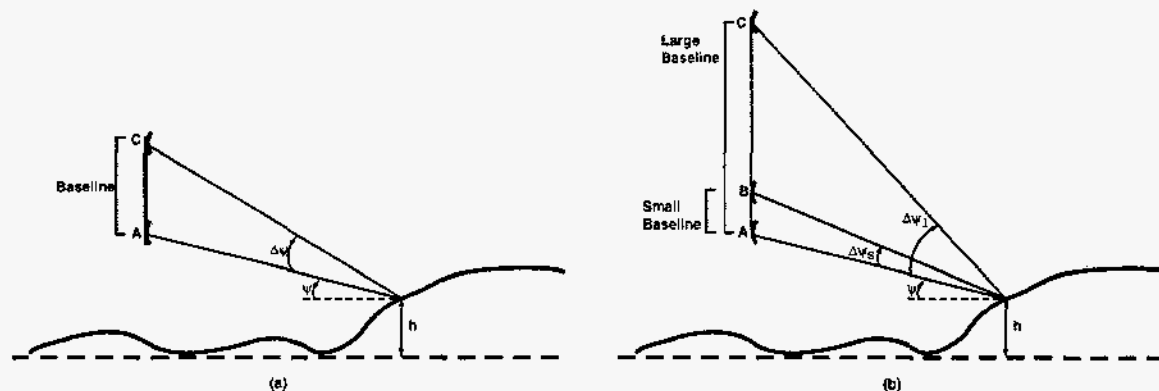


Figure 1: Configuration of SAR interferometers. a) Conventional using two phase centers, b) Three phase centers

will develop here employs the phase difference data from the small baseline formed by phase centers A and B, denoted by  $\phi_s$ , as well as the corresponding phase difference from the large baseline (formed by phase centers A and C), denoted by  $\phi_l$ . By limiting the size of the small baseline, we can ensure that the fringe data  $\phi_s$  have maximum and minimum phase values that differ by less than a full cycle, i.e., less than  $2\pi$  radians. Therefore, we can construct a terrain height estimate without use of any phase unwrapping whatsoever. The resulting terrain map tends to be of low quality, since the estimated

height accuracy is directly proportional to the size of the baseline. However, if the errors in the small baseline elevation map are not too large relative to the height associated with one cycle of phase of the large baseline data, then the small baseline height estimates can be used to place the large baseline phase data on their proper cycle, so that the  $2\pi$  ambiguities are resolved. Stated another way, the small baseline heights can be used to "seed" the more accurate estimates from the large baseline data without having to invoke any form of traditional phase unwrapping.

Previous work discussed the use of multiple baselines in SAR interferometry<sup>2</sup>, but did not describe the algorithm developed here nor did it demonstrate the performance advantages over traditional two-dimensional phase unwrapping. The algorithm that we propose here for SAR interferometry has been employed previously in other interferometric applications. In 1981, Jacobs and Ralston<sup>3</sup> discussed the general problem of direction-of-arrival determination in three-dimensions using a four-antenna array. That is, two angles (azimuthal and inclination) are estimated. They showed that the addition of a fifth antenna element gives rise to short and long baseline phase data that may be combined without use of conventional phase unwrapping. In 1994, Xu et. al.<sup>4</sup> proposed the basic three-phase center algorithm discussed here for IFSAR, but did not quantify nor demonstrate its performance. More recently, Zhao, Chen, and Tan<sup>5</sup> showed that the same concept could be applied to the problem of three-dimensional object shape measurement (profilometry) in laser interferometry.

## 2. PHASE ESTIMATION USING THREE PHASE CENTERS

The mathematics that describe the new phase estimation scheme are relatively simple. The diagram shown in Figure 2 describes the relationship between height and phase for the small and large baselines. The small baseline is chosen such that the range of terrain elevation heights in the scene imaged is less than the height,  $h_{max}$ , which corresponds to a full cycle of interferometric phase change. In this case, no phase unwrapping whatsoever is required to obtain the height estimate as:

$$\hat{h}_s = a_s \hat{\phi}_s \quad (1)$$

where  $a_s$  is the phase-to-height scale factor for the small baseline, given by<sup>1</sup>:

$$a_s = \frac{\lambda \cos \psi}{4\pi \Delta\psi_s} \quad (2)$$

In the above expression for  $a_s$ ,  $\Delta\psi_s$  is the depression angle difference represented by the small baseline (see Figure 1b). An expression for  $h_{max}$  is then given by:

$$h_{max} = 2\pi a_s = \frac{\lambda \cos \psi}{2 \Delta\psi_s} \quad (3)$$

The deviation of the estimation error for  $\hat{h}_s$  in Equation 1 is given by:

$$\sigma_s = a_s \sigma_\phi \quad (4)$$

Here,  $\sigma_\phi$  is the deviation of the interferometric phase estimate,  $\hat{\phi}_s$ , which is obtained from the pair of complex SAR images formed from the two phase centers. The estimator for  $\phi_s$  at a given point ( $m, n$ )

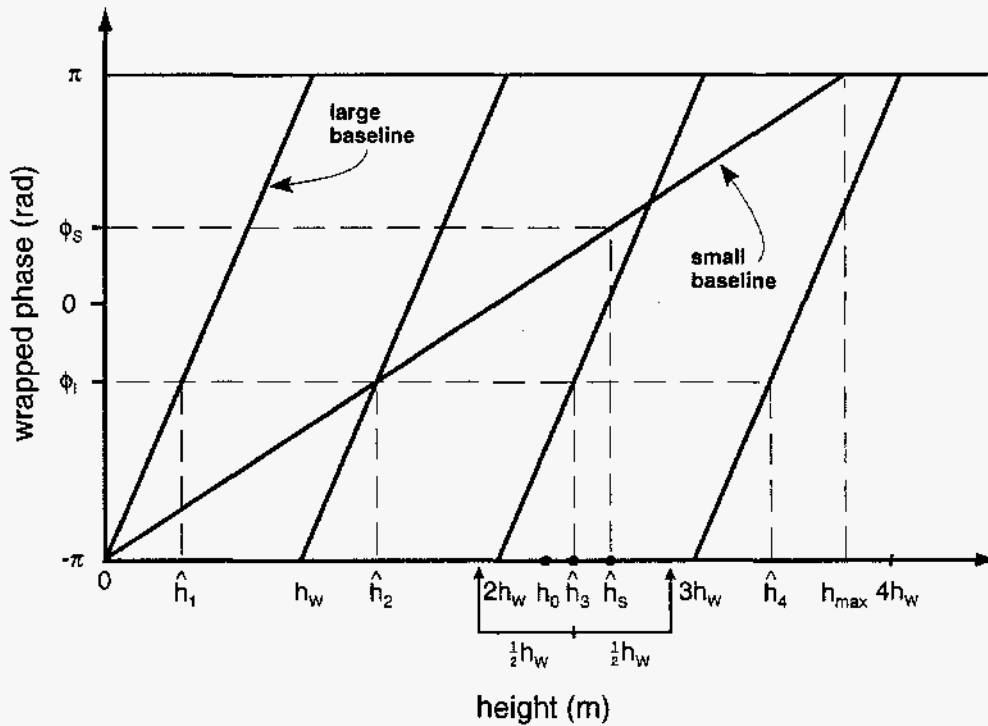


Figure 2: Interferometric wrapped phase vs. height for three-phase-center IFSAR. Actual height is  $h_0$ ; height estimates from large baseline are  $\hat{h}_1, \hat{h}_2, \dots$ ; height estimate from small baseline is  $\hat{h}_s$ ; wrapping height for large baseline is  $h_w$ ; wrapping height for small baseline is  $h_{max}$ . Jump cycle errors occur whenever  $|\hat{h}_s - \hat{h}_k| > h_w/2$ .

in the image is given by the expression:

$$\hat{\phi}_s = \mathcal{L} \left\{ \sum_{(i,j) \in A} f_{m+i,n+j}^* g_{m+i,n+j} \right\} \quad (5)$$

where the complex SAR images are denoted by  $f$  and  $g$ , and the symbol  $\mathcal{L}$  is used to indicate the argument (angle) of the complex quantity. The summation is performed over a local neighborhood of pixels,  $A$ , surrounding the pixel  $(m, n)$  for which  $\hat{\phi}_s$  is sought. Generally, this summation results in phase noise reduction at the expense of spatial resolution loss. It can be shown<sup>1</sup> that the above estimator for IFSAR phase is maximum likelihood (ML) and under reasonably general conditions, it is unbiased and Gaussian with variance prescribed by the Cramer-Rao lower bound:

$$\sigma_{\phi}^2 = \frac{1}{N \cdot \text{CNR}} \quad (6)$$

where  $N$  is the number of samples included in the neighborhood  $A$  of Equation 5, and CNR is the clutter-to-receiver noise ratio of the SAR images.

The problem in SAR interferometry is that if the baseline is chosen sufficiently small such that no phase unwrapping is required, then the resulting height estimation error deviation given by Equation 4 is unacceptably large. The large baseline phase data of the three phase center design (formed from

phase centers A and C in Figure 1b), however, have the potential to yield high accuracy terrain profile estimates, since the phase-to-height scale factor is proportionately smaller. That is, analogous to Equations 1 through 4, we have for the large baseline data:

$$\hat{h}_l = a_l \hat{\phi}_l \quad (7)$$

$$a_l = \frac{\lambda \cos \psi}{4\pi \Delta \psi_l} \quad (8)$$

$$h_w = 2\pi a_l = \frac{\lambda \cos \psi}{2 \Delta \psi_l} \quad (9)$$

$$\sigma_l = a_l \sigma_\phi \quad (10)$$

Here we have used the notation  $h_w$  for the height at which the large baseline "wraps", i.e.,  $h_w$  is analogous to the quantity  $h_{max}$  (Equation 3) for the small baseline data. Figure 2 shows that multiple solutions are possible for the height estimate from the large baseline phase measurement,  $\hat{\phi}_l$ , since  $h_w < h_{max}$ . The solutions are denoted as  $\hat{h}_1, \hat{h}_2, \hat{h}_3, \dots$ . The algorithm we propose for selecting the correct large baseline estimate, i.e., resolving the ambiguity, is to simply choose that  $\hat{h}_k$  for which the distance to the small baseline height estimate,  $\hat{h}_s$ , is smallest. This is essentially the projection method discussed by Xu, et. al.<sup>4</sup>

With a certain probability, of course, the above strategy for obtaining the correct  $\hat{h}_k$  will yield the wrong answer, i.e., the estimate will be one cycle lower or higher than the correct cycle. The probability of occurrence of such an error is easily calculated using the framework developed above. As shown in Figure 2, an error will occur whenever the distance between the small baseline height estimate and the correct large baseline estimate is greater than one half of the wrapping height associated with the large baseline. That is, the condition for a jump cycle error is given by:

$$|\epsilon| > \frac{h_w}{2} \quad (11)$$

where:

$$\epsilon = \hat{h}_s - \hat{h}_k \quad (12)$$

In Equation 12,  $\hat{h}_k$  is interpreted to mean the large baseline estimate on the correct cycle. Using the relationships defined in Equations 1 - 10, we can derive an expression for the probability of a jump cycle error. We assume that the probability density function for  $\epsilon$  is Gaussian<sup>1</sup>, with the variance of  $\epsilon$  equal to the sum of the variances of  $\hat{h}_s$  and  $\hat{h}_k$ . We then have:

$$p_\epsilon(\epsilon) = \frac{1}{\sqrt{2\pi}\sigma_\epsilon} \exp\left\{-\frac{\epsilon^2}{2\sigma_\epsilon^2}\right\} \quad (13)$$

with:

$$\sigma_\epsilon^2 = \sigma_s^2 + \sigma_l^2 \quad (14)$$

<sup>1</sup>A justification for this assumption stems from the fact that the phase estimator of Equation 5 is ML, and that all ML estimates are asymptotically Gaussian. In this case, we can invoke the property for reasonably large CNR values.

The probability of the condition of Equation 11 is then given by:

$$P_{jump} = 2 \int_{\frac{h_w}{2}}^{\infty} p_{\epsilon}(\epsilon) d\epsilon = 2 - 2 \operatorname{erf} \left( \frac{h_w}{2\sigma_{\epsilon}} \right) \quad (15)$$

where we use the following definition of the inverse error (erf) function:

$$\operatorname{erf}(x) = \frac{1}{\sqrt{2\pi}} \int_0^x \exp(-x^2/2) dx \quad (16)$$

Using the expression for  $h_w$  in Equation 9, we can rewrite Equation 15 as:

$$\begin{aligned} P_{jump} &= 2 - 2 \operatorname{erf} \left[ \frac{2\pi a_l}{2\sqrt{\sigma_s^2 + \sigma_l^2}} \right] \\ &= 2 - 2 \operatorname{erf} \left[ \frac{1}{2\gamma \sqrt{1 + \beta^2}} \right] \end{aligned} \quad (17)$$

In Equation 17 above,  $\gamma$  is the system phase noise level, expressed as a fraction of a full cycle, and  $\beta$  is the ratio of the large and small baselines, i.e.:

$$\gamma = \frac{\sigma_{\phi}}{2\pi} \quad (18)$$

$$\beta = \frac{a_s}{a_l} = \frac{\Delta\psi_l}{\Delta\psi_s} \quad (19)$$

### 3. SIMULATION RESULTS

In this section we show how the new three phase center algorithm works on a set of simulated IFSAR images. Figure 3 shows a real detected SAR image of some desert terrain, where the radar platform is flying along the right edge of the image, i.e., the range dimension is horizontal, with near-range to the right. Figure 4 shows a three-dimensional rendering of the actual terrain height profile that underlies this scene. Three SAR images are constructed to simulate collections from three phase centers, where the ratio of the large to small baselines is 20. Receiver noise was added to each of the three images with a CNR value of 9 dB. Interfering the small baseline image pair produces the fringe map of Figure 5. Notice that by design, all of the terrain relief is encoded into a single cycle of phase, i.e., multiple fringes do not appear. (Actually, due to receiver noise, some multiple cycle data do appear in the shadowed region on the left side of the image.) Figure 6 shows the fringe map that is constructed from interfering the large baseline pair.

Figure 7 and Figure 8 show the results of a two-dimensional phase unwrapping procedure applied to the large baseline data. The unwrapping algorithm used here is that of Flynn<sup>6</sup>, which employs a mask derived from the quality of the correlation between the two images. The unwrapping paths are not allowed to cross any portion of the mask, as the mask attempts to predict areas of the image wherein

phase discontinuities may exist. Whenever the mask either fails to cover a true phase discontinuity or gives indication of discontinuities which really do not exist, the output of the unwrapper is subject to errors. The mask derived from the simulated data is shown in Figure 7, while Figure 8 shows the rendering of the terrain height estimate produced by the unwrapper. Comparison of this rendering with that of the true terrain profile of Figure 2 indicates that the unwrapping algorithm has failed to adequately track the terrain over the steep sides of the mesa. The sides of the mesa are estimated to be significantly steeper than they really are. In addition, the height of the plateau on the left edge of the image is incorrectly estimated by an amount equivalent to three cycles of phase.

The results of the three phase center algorithm are more favorable in this case, as indicated by the renderings of Figures 9 and 10. Figure 9 is the direct output of the algorithm. Note that numerous spikes appear in the estimate, representing a significant number of jump cycle errors. Since the CNR for these images is 9 dB, the estimated number of jump cycles for this case (Equation 17) is large. Although the estimated height profile is unacceptable with this large number of spikes, the jump cycle errors can be nearly totally mitigated by use of non-linear filtering. Figure 10 shows the result of a 3 x 3 median filter applied to the estimate of Figure 9. Note the excellent fidelity between the filtered estimate and true profile of Figure 2.



Figure 3: Detected image

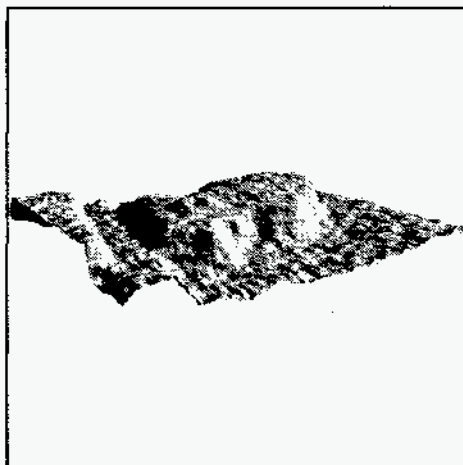


Figure 4: Rendering of terrain height profile

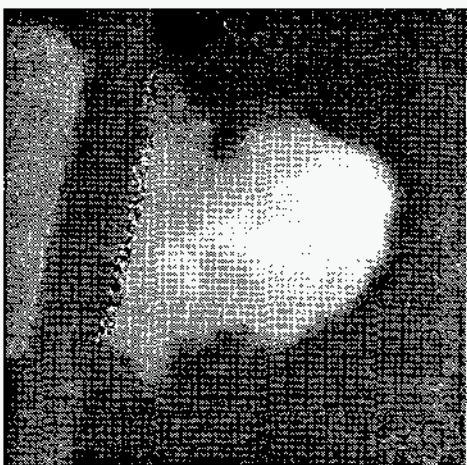


Figure 5: IFSAR fringe map formed from small baseline data

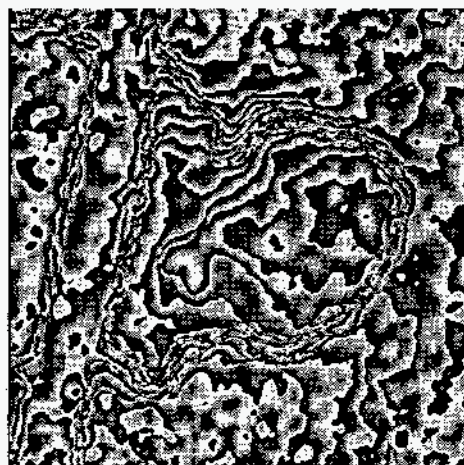


Figure 6: IFSAR fringe map formed from large baseline data





Figure 7: Mask used in 2-D phase unwrapping procedure

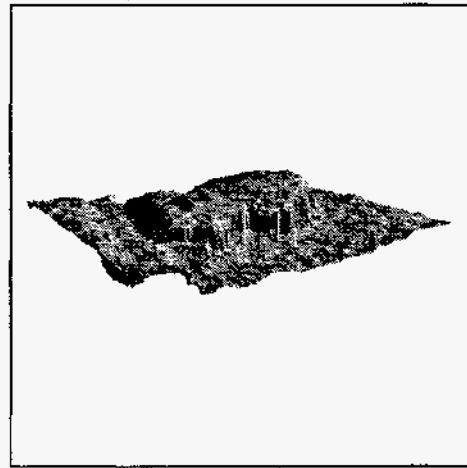


Figure 8: Rendering of terrain height estimate produced by 2-D phase unwrapping

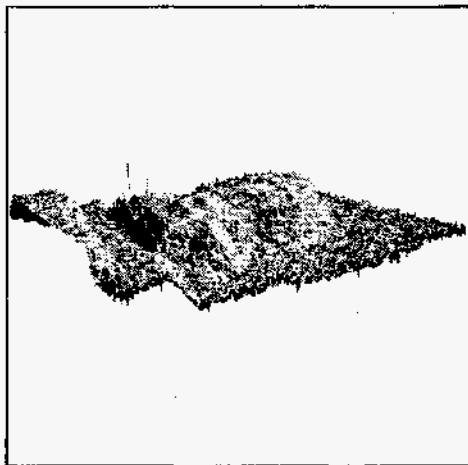


Figure 9: Rendering of terrain height estimate produced by 3-phase center technique, without median filtering

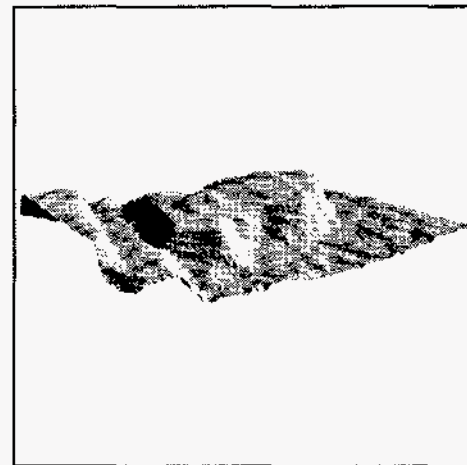


Figure 10: Rendering of terrain height estimate produced by 3-phase center technique, with median filtering

#### 4. SUMMARY AND CONCLUSIONS

We have demonstrated that use of three phase centers in SAR interferometry can lead to a terrain height reconstruction algorithm that avoids some of the pitfalls of traditional two-dimensional phase unwrapping of data from a pair of phase centers. By choosing one of the baselines to be sufficiently small (phase centers close together) that a single cycle of phase encodes the maximum terrain height extent, a coarse elevation estimate can be made that does not require any phase cycle ambiguity resolution. This estimate is then used to predict the proper cycle number for the larger baseline (phase centers far apart) phase difference data. The chief advantage of the new approach is that errors in cycle number are localized in the image. This is not the case for typical two-dimensional phase unwrappers, wherein errors can be propagated to entire regions of the image.

#### 5. ACKNOWLEDGMENTS

The authors would like to thank their colleague, Tom Flynn, who contributed to useful discussions and review of this paper. In addition, thanks to Perry Gore who produced the figures.

#### 6. REFERENCES

1. C. V. Jakowatz, Jr., et al, **Spotlight Mode Synthetic Aperture Radar: A Signal Processing Approach**, Kluwer Academic Publishers, Boston, 1996.
2. D.C. Ghiglia and D.E. Wahl, "Interferometric synthetic aperture radar terrain elevation mapping from multiple observations," *IEEE Sixth DSP Workshop*, Yosemite National Park, CA, Oct. 2-5, 1994.
3. E. Jacobs and E. Ralston, "Ambiguity resolution in interferometry", *IEEE Trans. AES*, AES-17, No. 6, Nov. 1981.
4. W. Xu, E. C. Chang, L. K. Kwok, H. Lim, W. C. A. Heng, "Phase-Unwrapping of SAR interferograms with multi-frequency or multi-baseline," *IGARSS 1994*, pp. 730 - 732.
5. H. Zhao, W. Chen, and Y. Tan, "Phase-unwrapping algorithm for the measurement of three-dimensional object shapes", *Applied Optics*, Vol. 33, No. 20, 10 July, 1994.
6. T. J. Flynn, "Consistent 2-D phase unwrapping guided by a quality map", *IGARSS 96*, Lincoln, Nebraska, 27-31 May, 1996.

#### **DISCLAIMER**

This report was prepared as an account of work sponsored by an agency of the United States Government. Neither the United States Government nor any agency thereof, nor any of their employees, makes any warranty, express or implied, or assumes any legal liability or responsibility for the accuracy, completeness, or usefulness of any information, apparatus, product, or process disclosed, or represents that its use would not infringe privately owned rights. Reference herein to any specific commercial product, process, or service by trade name, trademark, manufacturer, or otherwise does not necessarily constitute or imply its endorsement, recommendation, or favoring by the United States Government or any agency thereof. The views and opinions of authors expressed herein do not necessarily state or reflect those of the United States Government or any agency thereof.